

Vascularization and Adipogenesis of a Spindle Hierarchical Adipose-Derived Stem Cell/Collagen/ Alginate-PLGA Construct for Breast Manufacturing

Xiaohong Wang, Jiayin Wang

Abstract—The creation of vascularized adipose tissues is a subject of broad fundamental and technological interest in implantable breast manufacturing. Here, we demonstrated a simple, easy, and effective way to fabricate a spindle hierarchical poly(DL-lactic-co-glycolic acid) (PLGA) encapsulated adipose-derived stem cell (ADSC)/collagen/alginate construct with a multiple-branched vascular network using a rotational combined mould system (RCMS). Both the optimized PLGA overcoat and internal collagen/alginate hydrogel provided the ADSCs with a stable and comfortable accommodation to grow, proliferate, and differentiate. Cell viability remained at a comparatively high level during 4 weeks in vitro engagement with two groups of cell growth factor combinations. At the end of the second week, part of the cells were engaged into endothelial cells, while at the end of the fourth week more than 63% of the ADSCs were replaced by adipose cells. We envisage that this RCMS, vascularization and adipogenesis techniques will provide an enabling platform for a wide array of research and clinical applications.

Keywords—Vascularization; adipogenesis; a rotational combined mould system; adipose-derived stem cells (ADSCs); collagen/alginate hydrogel.

I. INTRODUCTION

Breast losses have caused a great deal of mental and physical handicaps for patients due to congenital dysplasia, tumor resection, traumatic injuries and other reasons [1]. Breast manufacturing with large quantities of adipose tissue and intensive blood vessels have attracted more and more attentions over the last two decades. Two essential issues must be addressed for breast manufacturing: one is to establish a vascular network in a three-dimensional (3D) construct, the other is to incorporate adipose cells on the vascular network [2-4]. Particularly, stem cell vascularization and adipogenesis are two promising aspects for breast equivalent reconstruction. A protocol that accurately recapitulates the stem cell physical and biological environment is fundamentally and urgently needed to improve our understanding of complex breast manufacturing.

Manuscript published on 30 January 2015.

*Correspondence Author(s)

Prof. Xiaohong Wang, Department of Mechanical Engineering, Tsinghua University, Beijing 100084, P.R. China.

Mr. Jiayin Wang, Department of Mechanical Engineering, Tsinghua University, Beijing 100084, P.R. China.

© The Authors. Published by Blue Eyes Intelligence Engineering and Sciences Publication (BEIESP). This is an [open access](http://creativecommons.org/licenses/by-nc-nd/4.0/) article under the CC-BY-NC-ND license <http://creativecommons.org/licenses/by-nc-nd/4.0/>.

It is generally accepted that a vascular network plays a critical role in cell survival and tissue remodeling in the field of complex organ manufacturing [5-7]. In the absence of a perfusable vascular network, 3D construct densely populated with cells would quickly develop a necrotic core [8], because cells cannot survive further than several hundred microns away from blood vessels [9]. Yet the lack of a general approach to rapidly build such networks remains a major challenge for complex organ manufacturing [10]. Several groups have focused on the creation of branched vascular networks using different technologies, such as soft lithography [11], direct-write assembly [12], additive manufacturing (AM, also named as rapid prototyping RP, or three-dimensional printing 3DP) [13], laser ablation [14]. In our previous studies, a bifurcating vascular bed with round internal channels was fabricated using single or double nozzle RP deposition techniques [15,16]. The RP enabling techniques allow the facile construction of complex architectures at the right time at various ambient conditions. However, these technologies have been thus far limited to one or two cell-laden biomaterials with a simple branched vascular system. The primarily reason is the technical constrains in providing multiple nozzle RP equipments within a short time [17,18]. We and others have demonstrated that each of the available techniques has intrinsic limitations in complex organ manufacturing [19,20].

On the other hand, due to the unique conditions of stem cell growth, proliferation and differentiation, vascularization and adipogenesis of the branched channel networks have become two of the hot topics over the world. Especially in scalable large 3D constructs, vascularization means forming new intact blood vessels by endothelial cells or endothelial precursor cells [21]. There is a rush of new approaches for tissue vascularization and adipogenesis. For example, Stoppato and coworkers created a poly(D,L-lactic acid) (PDLLA) and silk fibroin fiber scaffold to better support endothelial cell colonization and in vivo vascularization [22]. Sahota and coworkers put a biodegradable scaffold into nude mice to reconstruct a human skin containing autologous keratinocytes, fibroblasts, and endothelial cells [23]. A little earlier before, Laschke and coworkers implanted a polyurethane scaffold into dorsal skinfold chambers of BALB/c mice to study the vascularization processes using an intravital fluorescence microscopy [24]. Adipose-derived stem cells (ADSCs), which exist in adipose tissue, can be easily collected from humans or animals by a simple liposuction method.

ADSCs can differentiate into many kinds of somatic cells, such as osteoblasts, neurons and endothelial cells. For this reason ADSCs could be the most potential cellular source for vascular and adipose tissue engineering [25]. Laschke and coworkers seeded adipose-derived mesenchymal stem cells into a porous polyurethane scaffolds in order to achieve blood vessel formation [26]. While most of the literatures included the use of medium containing fetal bovine serum for endothelial differentiation, Konno and coworkers developed a method for differentiating mouse adipose tissue-derived mesenchymal stem cells into vascular endothelial cells under serum-free conditions [27].

Here we present a simple, easy, and effective approach to manufacture complex organ precursors with a controllable spindle hierarchical architecture, a predefined vascular network and a multiple cell type differentiation environment. ADSCs from a mouse were used as the vascularization and adipogenesis cell source. A mixture of collagen and alginate hydrogel was used to locate the stem cells. A rotational combined mould system (RCMS), consisting of a basement mould, an internal branched mould and an external mould, permits many sophisticated applications come true in a single construct. This is the first report of this brand-new technique has been used in complex organ, such as the breast, manufacturing.

II. METHODS

A. Adipose-Derived Stem Cells

All animals were raised according to the principles of laboratory animal care and guidance (www.people.com.cn) for the care and use of laboratory animals in China. ADSCs were isolated from Sprague Dawley (SD) rat (120-150 g, Beijing University Medical Center of Laboratory Animals) subcutaneous adipose tissue. The tissue was excised, washed by a series of betadine dilutions, degreased, and minced before digested in a 0.075% Type II collagenase (Sigma, St. Louis, MO, US) solution at 37°C for thirty minutes. After centrifugalization ADSCs were separated from adipocytes and other tissue fractions through a 100 mm cell strainer and cultured in Dulbecco's modified Eagle's medium (DMEM, Gibco, Santa Cruz, CA, US) with the addition of 15% fetal bovine serum (FBS) at 37°C and 5% CO₂. The cells were grown to subconfluence and passed by standard trypsinization methods.

B. Preparation of the ADSC/Collagen/Alginate Mixture

Type I collagen (Sigma, St. Louis, MO, US) was diluted in DMEM at a concentration of 20 mg/mL. Sodium alginate (Sigma, St. Louis, MO, US) was dissolved in phosphate-buffered saline (PBS) at concentrations of 0.7%, 1.3%, 2.5%, 5% (w/w) and sterilized. Equal volumes of collagen and alginate solutions were mixed thoroughly. The pure collagen (20 mg/mL) and alginate (5% (w/v)) solutions were used as controls. The pH of the collagen/alginate mixture was adjusted to 7.2 using 0.1 mol/L NaOH solution [28]. After the collagen, collagen/alginate and alginate hydrogel being washed three times with PBS, they were dehydrated following the concentration gradient: ethanol in PBS 50%, 70%, 80%, 90%; 100% ethanol; ethanol in tert-butyl alcohol 50%; 100% tert-butyl alcohol. Then put the samples in tert-butyl alcohol at -20°C. After dehydration, the

samples were freeze-dried and examined using a scanning electron microscopy (SEM), (Hitachi S-450, Japan). ADSCs (passage 4-6) acquired by standard trypsinization methods were suspended in the collagen/alginate solution with a density of 1×10^6 cells/mL before the following experiments.

C. Mechanical Property and Permeability Tests of the PLGA Films

Synthetic PLGA (Mw 100,000 Dalton, brought from the Institute of Medical Devices of Shandong Province, China) was dissolved into tetraethylene glycol with three different concentrations (10%, 15%, 20% w/v). Tensile and compression properties of three PLGA films with concentrations of 10%, 15%, and 20% (w/v) were measured using a universal testing machine (Zwick Materials Testing BZ005/TN2S). PLGA samples for mechanical testing were formed by a set of custom made moulds to attain standard sample shapes. Tensile samples were made into standard tensile sample shape, ribbon-like pattern with small width in the middle. The samples were averaging $25 \times 10 \times 1.5$ mm³ in boundary dimensions and averaging 8×1.5 mm² in the sectional dimension which snapped in the middle, the compression speed was 1 mm/min. Permeability ability was tested by measuring a 3% acetic acid solution permeating the PLGA film time with a pH test strip at the bottom.

D. Fabrication of the Spindle Hierarchical ADSC/Collagen/Alginate-PLGA Construct Using a RCMS

A RCMS was used to construct the cell-laden collagen/alginate and PLGA biomaterials into 3D constructs. As shown in Fig. 1, the RCMS consists of three parts: an upper cylindrical polytetrafluoroethylene mould with a central hole in the top wall, a basement mould with 7 holes on the bottom, and an internal branched mould with a bunch of 7 polyethylene wires (1.2 mm in diameter). The 3D cell-laden constructs were made by several steps. Firstly, the 7 ends of the internal branched mould were inserted separately to the 7 holes on the bottom of the basement mould. The upper cylindrical mould was put onto the basement mould. The upper internal branched and cylindrical moulds were rotated at certain speed, such as 10 r/min, 20 r/min, 30 r/min, 40 r/min and 50 r/min. Secondly, the ADSC/collagen/alginate mixture was injected into the cavity of the combination moulds through the upper central hole. After the ADSC/collagen/alginate mixture was filled and climbed out the cavity, a 3% (w/v) CaCl₂ solution was injected along the internal branched mould. The sodium alginate was crosslinked and the ADSC/collagen/alginate mixture was become a semi-spindle shape due to Weissenberg effect of non-Newtonian fluid. Thirdly, after the upper cylindrical and basement moulds were removed, two identical semi-spindle constructs with the internal branched mould were jointed together with a layer of the ADSC/collagen/alginate mixture. After the spindle construct was coated with a layer of PLGA solution, the internal branched moulds were pulled out from the gelled ADSC/collagen/alginate hydrogel. Then the whole construct was immediately immersed in PBS to extract the tetraethylene glycol solvent in the PLGA overcoat.

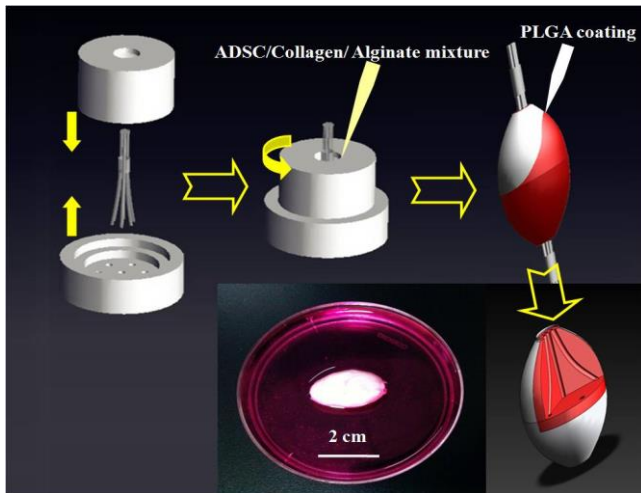


Fig. 1 Construction processes and the internal/external structures of the spindle hierarchical ADSC/collagen/alginate-PLGA construct

E. Engagement of the ADSCs to Endothelial and Adipose Cells

After being cultured in the DMEM with 10% FBS for 2 days, the constructs were switched to endothelial growth factor containing DMEM supplemented with 50 ng/mL vascular endothelial growth factor (VEGF, PEPRO TECH, Rocky Hill, NJ, US), 3 ng/mL TGF- β 1 (PEPRO TECH, Rocky Hill, NJ, US) polyclonal antibody and 10 ng/mL basic fibroblast growth factor (b-FGF, PEPRO TECH, Rocky Hill, NJ, US). The culture medium was changed every two days.

After 11 days of engagement with the endothelial growth factor containing culture medium, the constructs were further switched to adipogenic growth factor containing DMEM with the addition of 15% FBS, 1 μ M insulin, 1 μ M dexamethasone, 50 u/mL aprotinin and 0.5 mmol/L isobutyl-methylxanthine (IBMX; Sigma) at 37°C and 5% CO₂ environment for 14 days.

F. Scanning Electron Microscope Observation

At the day of 3, 7, 14, the cell-laden constructs with a PLGA shell were fixed with 5% glutaraldehyde for 4 h before dehydrated in a graded ethanol series, sputter-coated with gold after freeze-dried and finally observed using a FEI Quanta 200 scanning electron microscope (SEM), (Hitachi S-450, Japan).

G. Cell activity

3-(4,5)-dimethylthiaziazolo (-z-y1)-3,5-diphenyltetrazolium bromide (MTT, Zhongshan Company, China) assay was used to measure cell proliferation rate in the constructs. The constructs were cut into small pieces before they were put into a 96-welled plate with 10 μ L 5 mg/mL MTT solution and incubated at 37°C for 4 h [29]. 100 μ L of dimethyl sulfoxide (DMSO) was injected to each sample and the samples were shaken for 10 min. A Bio-Rad 550 reader (Japan) was used to measure the optical density (OD) of each sample.

H. Fluorescence Staining

At the day of 3, 7, 14, 21, some of the constructs were sliced and stained with 30 μ g/mL acridine orange (AO, Sigma) and 50 μ g/mL propidium iodide (PI, Sigma) solutions for 10 min at 37°C before being washed with PBS three times [30]. The samples were observed with a laser scanning confocal microscope (LSCM, Zeiss, LSM710, Germany). Samples for

immunofluorescence staining were first soaked in 4% glutaraldehyde for half an hour, and washed 3 times with PBS. Then primary antibodies (rabbit anti-facVIII, BMASSAY, Beijing, China) were added and the samples were incubated at 37°C for 12 h. After the samples were washed with PBS for 5 min, a second antibody (AffiniPure goat anti-rabbit IgG (H+L) rhodamine (TRITC)-conjugated, BMASSAY, Beijing, China) was added and the samples were incubated for 3 h before being washed with PBS for 5 min. To stain the cell nucleus, the samples were further incubated with 4',6-diamidino-2-phenylindole (DAPI, BMASSAY, Beijing, China) for 10 min before being examined with the LSCM. Slices (50 μ m in thickness) of the constructs in radial direction were stained with Oil Red O to measure neutral lipid and fat accumulation. Simply, the samples were put in absolute isopropyl alcohol for 5 min before being stained with pre-warmed and filtered Oil Red O solution at 60°C for 10 min. After being put in 85% propylene glycol solution for 3 min, and rinsed with distilled water twice, the samples were stained with mayer's hematoxylin for 1 min, washed thoroughly, and mounted with glycerin jelly before being examined under a microscope. The red stained and total cell numbers were counted. The optical density (OD) of the solution was measured as well using an ELISA reader (Nicesound Electronics Co., Ltd) for the purpose of quantitative analysis.

III. RESULTS

A. Optimal Choice of the PLGA Concentration

There are two purposes for the use of synthetic PLGA as an overcoat. One is to provide a mechanical support for the cell-laden collagen/alginate hydrogel with anti-press and anti-suture abilities. The other is to prevent the cell-laden hydrogel from dissolving in the culture medium too quickly and provide the cells with a stable environment to form tissues and organs. One out of the three given PLGA concentrations (i.e. 10%, 15%, 20% (w/v)) was comprehensively chosen according to the mechanical properties and permeability testing results. The tensile test results are shown in Fig. 2a. It is clear that the extension strength increased as the PLGA concentration rose. All the 10% (w/v) samples snapped below 0.75 N load or 200 KPa stress, while the 15% (w/v) samples were slightly increased, ranging from 0.9 N to 1.6 N, or 230 KPa to 450 KPa stress. The highest load that rendered 20% (w/v) samples was much higher than 2.6 N or 430 KPa. The compression test results are shown in Fig. 2b. Similarly, the higher the PLGA concentration is, the higher the compressive strength becomes. One notable exception is that the 20% (w/v) samples ended up at a quite low stain, maximum 3 mm. This result indicates that the higher the concentration is, the lower the tenacity becomes, which may cause the samples to collapse easily. The ultimate load and elongation of the samples were tested simultaneously. The ultimate load rose from 10% PLGA's 0.73 N to 20% PLGA's 2.6 N in tensile test and from 10% PLGA's 5.8 N to 20% PLGA's 9.2 N in compression test, respectively, along with the increase of the PLGA concentration.



Inversely the elongation figures dropped from 10 % PLGA's 7.2% to 20 % PLGA's 3.7%.

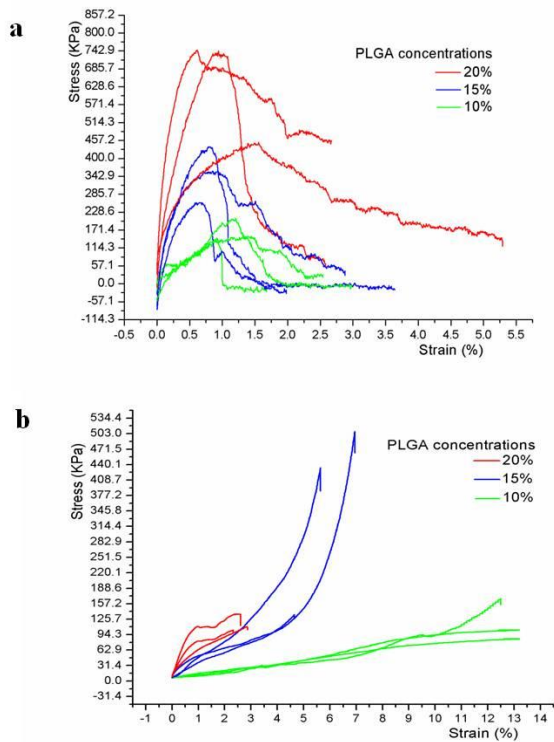


Fig. 2 Stress strain curves of the PLGA samples with different concentrations: (a) tensile test results, (b) compression test results

The permeability results of both the PLGA films with different concentrations and thickness are presented in Table 1. As either the concentration or thickness increased, it would take a longer time for the solution to permeate. Similar results were found for the collagen/alginate hydrogels with different 0.7%, 1.3%, 2.5%, 5% (w/v) alginate concentrations and a fixed 20 mg/mL collagen concentration. When the alginate concentration increased from 0.7% to 5% (w/v), the permeating time enhanced from 49 ± 0.5 s/mm to 220 ± 0.5 s/mm.

Table 1 Permeability results of the PLGA films

PLGA concentration	10 % (w/v)	15 % (w/v)	20 % (w/v)
PLGA thickness (mm) /	0.23/ 1.03/	0.27/ 0.37/	0.28/ 1.11/
Permeating time (s)	18 ± 1.0 / 106 ± 0.3 / 149 ± 1.2	17 ± 0.8 / 20 ± 0.3 / 26 ± 0.2	19 ± 0.5 / 45 ± 0.6 / 204 ± 1.1
	1.11/ 180 ± 0.6 / 1.22/ 193 ± 0.2	0.56/ 143 ± 0.4 / 0.97/ 198 ± 1.3	1.18/ 227 ± 0.5 / 1.95/ 427 ± 0.1

Compared the mechanical properties and permeabilities of the three concentrations of PLGA films, the 10% (w/v) PLGA was poor in both the tensile and compression strength tests. The 20% (w/v) PLGA was poor in both the tenacity and permeability. Based on the requirements in practical application, the 15% (w/v) PLGA with strong mechanical properties and above average permeability was chosen for the following coating experiments.

B. Optimal choice of the sodium alginate concentration

Morphologies of the internal collagen/alginate mixtures with the same collagen concentration (20 mg/mL) and different alginate concentrations (i.e. 5%, 2.5%, 1.3%, 0.7% (w/v)) after freeze-drying are shown in Fig. 3. In Fig. 3a and 3b the crosslinked pure alginate (5% (w/v)) and 5% (w/v) alginate/20 mg/mL collagen form thick collagen/alginate hydrogel, which appears in sheet-like structures with irregular micro- and macro-pores in between. The thick collagen/alginate hydrogel may encapsulate the cells tightly, which makes it not suitable for mass exchange among cells. In Fig. 3c, the number of micropores in the 2.5% (w/v) alginate/20 mg/mL collagen sample is significantly higher and the average micropore size is much smaller than those in Fig. 3a and 3b. In Fig. 3d and 3e, clear and regular micropore distributions were detected with 1.3% and 0.7% (w/v) alginate concentrations. The average pore size is further reduced in the pure collagen sample (Fig. 3f). Some of the alginate/collagen hydrogel properties could be reflected by the SEM pictures. The group with 1.3% alginate solution was chosen for the following 3D construction experiments.

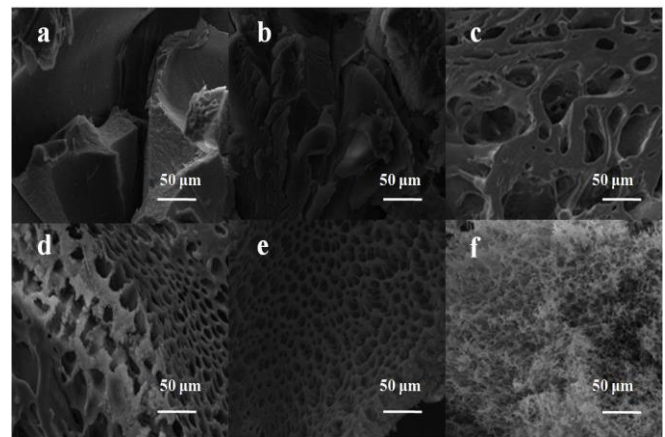


Fig. 3 Morphologies of the collagen/alginate hydrogel with a fixed 20 mg/mL collagen and different alginate concentrations: (a) pure alginate (5% (w/v)); (b) 5% (w/v)/collagen (20 mg/mL); (c) 2.5% (w/v) /collagen (20 mg/mL); (d) 1.3% (w/v) /collagen (20 mg/mL); (e) 0.7% (w/v) /collagen (20 mg/mL); (f) pure collagen (20 mg/mL)

C. Optimal Choice of the Rotation Speed of the RCMS

When the upper internal branched and cylindrical moulds were rotated at certain speed, such as 10 r/min, 20 r/min, 30 r/min, 40 r/min and 50 r/min, the cell-laden collagen/alginate hydrogel moved around the internal branched mould according to the Weissenberg effect of non-Newtonian fluid. After the alginate molecules were crosslinked with the CaCl₂ solution, the cell-laden collagen/alginate hydrogel took shapes. The rotation speed had a significant effect on the semi-spindle cell-laden collagen/alginate architectures. As shown in Fig. 4, when the rotation speed was fixed at 10 r/min, most of the cell-laden collagen/alginate hydrogel sited on the interval of the combined moulds with a thick cylinder structure.



As the speed went up, such as 20 r/min and 30 r/min, the climbing pole phenomenon was more and more obvious. The semi-spindle structures of the cell-laden collagen/alginate hydrogel were predominant. At 40 r/min and 50 r/min most of the cell-laden collagen/alginate hydrogel enclosed the internal branched mould with a slim semi-spindle structure.

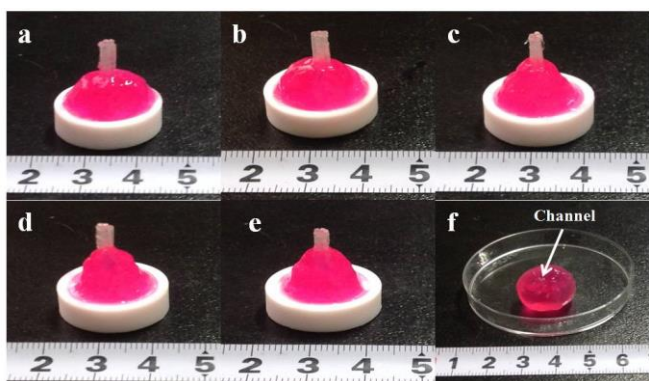


Fig. 4 Effects of rotation speeds and crosslinking on the semi-spindle cell-laden collagen/alginate hydrogel shapes: (a) 10 r/min; (b) 20 r/min; (c) 30 r/min; (d) 40 r/min; (e) 50 r/min; (f) a semi-spindle construct with the internal branched mould was removed from the cell-laden collagen/alginate hydrogel

In the semi-spindle ADSC/collagen/alginate-PLGA construct half a multi-branched vascular network was formed. When two of the semi-spindle constructs were integrated, a vascular network was created. This vascular network includes one inlet, 7 branched channels, and an outlet. Especially, when the branched daughter channels were not connected directly, a middle connected layer in the spindle ADSC/collagen/alginate-PLGA construct was formed. The PLGA overcoat acts as a protective shell for the cell-laden collagen/alginate hydrogel. Culture medium can pass through the inlet and outlet of the spindle construct.

D. Cell Viability in the Construct

After 2, 6, 13, and 20 days in vitro cultures and engagement, cells were stained with AO/PI and observed using a LSM (Fig. 5). The living cells appeared in green and dead cells in red color. Along the branched channel, there was nearly no red fluorescence from PI staining except the massive green fluorescence from AO staining in the day 3 samples (Fig. 5a). After 7 days engagement, sparse red PI fluorescence was detected which is surrounded by massive green fluorescence (Fig. 5b). In addition, a big red spot indicates that the cell died not long ago. Especially, few red spots appeared in the middle connected layer at day 14 (Fig. 5c). While a great deal of large cell aggregations were discovered with green fluorescence. However, some bright red fluorescence dots emerge in the day 21 samples (Fig. 5d), accompanied with far more green fluorescence. The AO/PI immunofluorescence staining results indicate the viabilities of the ADSCs at different in vitro culture and engagement periods. There was no dead cell in the first 2 days cultures before the growth factors were added. Few dead cells were found during the first 4 days angiogenic growth factor engagement. A few dead cells were detected during the other 7 days with angiogenic growth factor engagement. Many dead cells emerged during the 7 days adipogenic growth factor engagement after the 11 days angiogenic growth factor

engagement. During the 3 weeks in vitro culture and engagement period cell apoptosis occurred slowly through the later 2 weeks. The high cell viability over the first 3 weeks suggests that the 3D constructs are suitable for the ADSCs to grow, proliferate and differentiate. The internal collagen/alginate hydrogel and PLGA overcoat provided the cells with a stable and suitable survival accommodation.

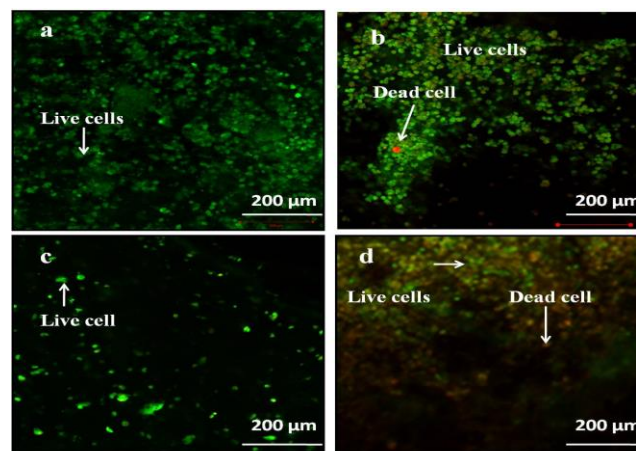


Fig. 5 Acridine orange/Propidium iodide (AO/PI) staining of the cells at different in vitro culture and engagement time points, (a) along the branched channel at day 3 before the growth factors being incorporated in the culture medium; (b) along the branched channel at day 7 with 4 days angiogenic growth factor engagement; (c) in the middle connected layer at day 14 with 11 days angiogenic growth factor engagement; (d) in the middle connected layer at day 21 with 11 days angiogenic growth factor and 7 days adipogenic growth factor engagement

MTT assay results are shown in Fig. 6. During the first 2 days in vitro culture ADSCs proliferated quickly in the 3D constructs. Follow that, cell proliferation rate speeded up in about one week and the cell number reached a considerably high degree. From day 7 to 14, cell proliferation rate slowed down and the cell number maintained an obviously high level, approximately 3 times as the original number. Two weeks later, the cell number decreased a little as a consequence of cell apoptosis and differentiations.

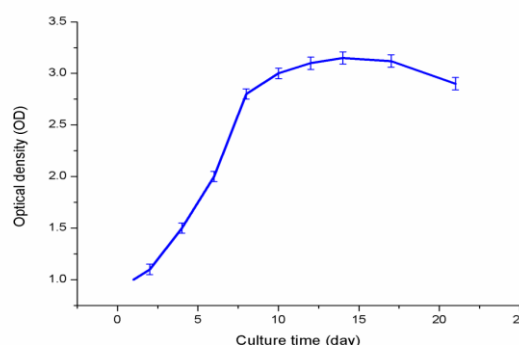


Fig. 6 MTT assay results of the cells in the 3D construct within 3 weeks of in vitro culture and engagement

E. Engagement of the ADSCs to Endothelial and Adipose Cells

Several LSM pictures are shown in Fig. 7. Besides the immunofluorescence staining for mature endothelial cells, all the samples were stained with 4',6-diamidino-2-phenylindole (DAPI) solution with easily distinguished blue cell nuclei. With the addition of angiogenic growth factors in the culture medium red fluorescence marker for mature endothelial cells appeared gradually (Fig. 7b, 7c and 7d). When the two branched daughter channels were not connected directly, a middle connected layer was formed with a little red fluorescence marker. This layer was easily to be induced into endothelial tissue with a capillary network (Fig. 7b) in less than one week of engagement. Most of the ADSCs deep inside the collagen/alginate hydrogel remained their original phenotypes. As time moved on, the red fluorescence spots increased and some cells around the channels linked together to form fiber like structures (Fig. 7c). Along the branched channels, the red fluorescence emerged alongside the blue spots (Fig. 7d). Especially, some of the endothelial like cells arranged in parallel mimicking the intima structure inside a blood vessel. At this stage, over 60% of the ADSCs located along the branched channels of the 3D constructs differentiated into endothelial cells. Meanwhile, cell differentiation rate deep inside the collagen/alginate hydrogel was relatively low.

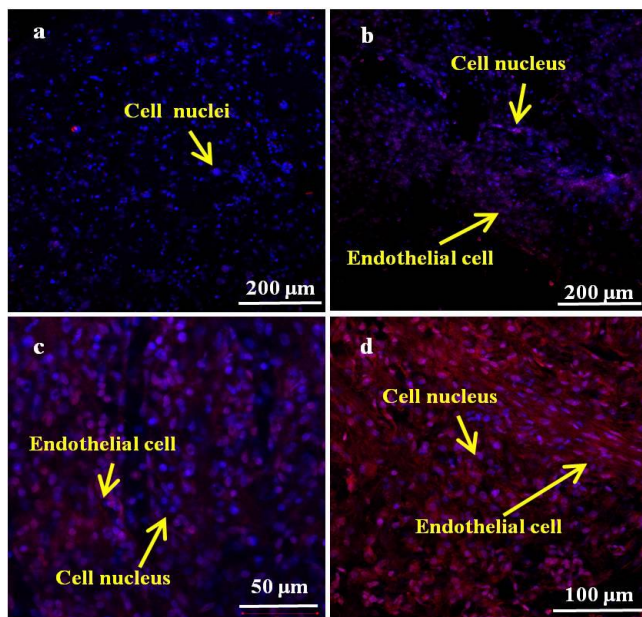


Fig. 7 Immunofluorescence observations of the factor VIII and DAPI staining results: (a) along the branched channel at day 3 before the growth factor engagement; (b) in the middle connected layer at day 7 with 4 days angiogenic growth factor engagement; (c) in the middle connected layer at day 14 with 11 days angiogenic growth factor engagement; (d) along the branched channel at day 21 with 11 days angiogenic growth factor and 7 days adipogenic growth factor engagement

Fig. 8 represents the oil red O staining results of the ADSCs differentiated into adipocytes after the adipogenic growth factors were added into the culture medium. The photos in Fig. 8a and Fig. 8b were taken at day 17 and day 21, respectively. There was no adipocyte appearance during the

first 14 days in vitro culture and engagement toward endothelial cells either along the branched channel or inside the middle connected layer. During the first two or three days engagement with adipogenic growth factors the adipogenic differentiation ratio was rather low especially along the channels where the ADSCs had differentiated into endothelial cells. The rate of the ADSCs differentiated into adipocytes accelerated since the fourth day with the presence of the adipogenic growth factors in the culture medium. This high differentiation rate lasted for two weeks, with more than 63% of the ADSCs differentiated into adipocytes at the end of the fourth week (Fig. 9). At this stage, less than 25% of the ADSCs remained endothelial cell phenotype. Prosperously differentiations of the ADSCs into both endothelial and adipose cells were obtained with different growth factor engagements.

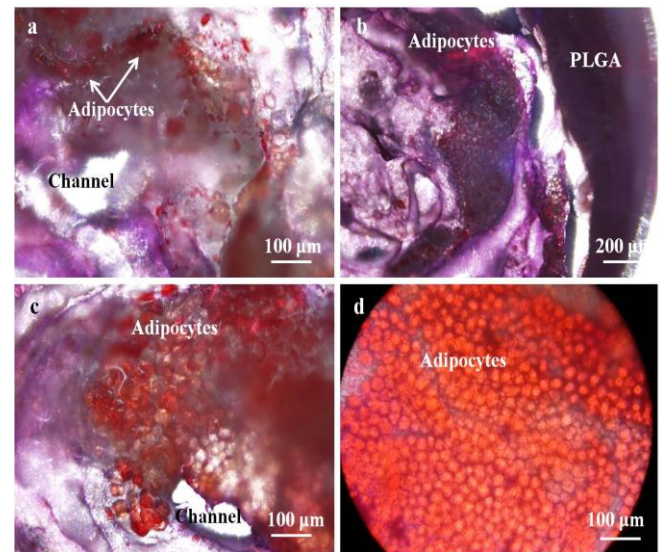


Fig. 8 Oil red O staining results of the adipocytes at different engagement time points: (a) along the branched channel at day 17; (b) along the branched channel at day 21; (c) along the branched channel at day 25; (d) in the middle connected layer at day 28

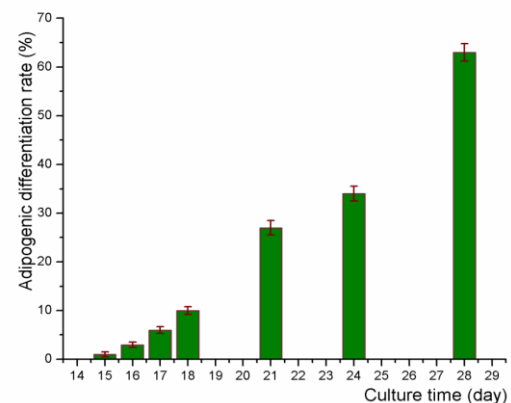


Fig. 9 Adipogenic differentiation rate since the addition of adipogenic growth factors in the DMEM at the fourteenth day for 14 days engagement

IV. DISCUSSION

Vascular adipose tissue construction with biocompatible materials, including non-immune patient derived cells, is one of the main objectives for complex breast manufacturing [2-4]. In the context of breast manufacturing, perhaps the least progress has been made is the development of a vascular system mimicking its native counterpart. Endothelial cells present an attractive target for both the promotion and inhibition of angiogenesis in a variety of clinical settings. Cocultures of endothelial cells with other functional cells in a natural hydrogel form interconnected networks that are reminiscent of capillary branches. Nonetheless, the formation of capillary networks in vitro remains a poorly characterized art [31]. It remains unclear how gel-cultures promote network formation, whether such networks are physiologically relevant and how to better define the culture system. Type I collagen and sodium alginate are natural polymers and offer numerous advantages in regenerative medicine with excellent biological properties [32,33]. Generally, these natural polymers have notorious poor mechanical properties especially when they were used as anti-stress or anti-suture biomaterials. On the contrary, synthetic polymers, such as PLGA and PU, hold excellent mechanical strengths [34-36]. In the present study we made use of their respective advantages of both natural (collagen and alginate) and synthetic (PLGA) polymers, to create a complex yet stable cell-laden construct for vascular breast regeneration. The collagen/alginate hydrogel acted as an ECM to provide the ADSCs with a comfortable accommodation. When the alginate molecules were crosslinked with CaCl₂ solution, the collagen molecules were entangled in the alginate molecules. The poor mechanical properties of the natural collagen/alginate hydrogel were improved. By coating the cell-laden collagen/alginate hydrogel with a synthetic PLGA overcoat the mechanical properties of the construct were further enhanced. With the aid of the RCMS, it was easy to form a semi-spindle cell-laden construct containing a multiple-branched vascular network due to the Weissenberg effect of non-Newtonian fluid. After the two semi-spindles were connected and coated with PLGA, a spindle construct with a branched vascular network was created. The ability to easily and tightly control the biological environments of the ADSCs enables the RCMS to be an ideal tool for quantitatively analyzing the vascular and adipose tissue regeneration processes (Fig. 1-2).

It is also discovered that the PLGA concentrations have great influence on the mechanical (tensile/compression) properties and permeabilities of the PLGA structures. The lower the concentration is, the higher the compression properties and quicker permeabilities are. The concentrations of the 10% and 20% (w/v) PLGA solutions were excluded either because of the poor mechanical properties or the lack of tenacity and permeability. The 15% (w/v) PLGA solution was chosen for the later construction experiments due to its strong mechanical properties and above average permeability. With the permeable PLGA overcoat, the multiple branched channels inside the cell-laden collagen/alginate hydrogel remained more than 4 weeks. With the branched vascular network and porous PLGA overcoat, nutrients/gases were easily transferred to the cells inside the construct. ADSCs therefore maintained a very high viability during the 4 weeks

in vitro culture and engagement stages. After a certain period of in vitro engagement with a cocktail angiogenic and adipogenic growth factors, ADSCs were partially replaced by endothelial cells and adipose cells according to their respective locations in the construct (Fig. 7-9). Especially on the surface of the internal branched channel, most of the ADSCs differentiated into endothelial cells during the first engagement stage.

It was also found that the quantity of the ADSCs tripled in the constructs after the first two weeks in vitro culture. To increase the cell density in the collagen/alginate hydrogel, the construct was first cultured in the FBS containing DMEM for two days before the growth factors were added. With the addition of endothelial growth factors (i.e. VEGF, TGF- β 1, and b-FGF) endothelial cell mark (red fluorescence) appeared gradually in the picture (Fig. 7). After two weeks engagement, the increased red fluorescence color indicates that most of the ADSCs, especially those along the branched channel surface, differentiated into endothelial cells. After the angiogenic growth factors (i.e. insulin, dexamethasone, aprotinin, and isobutyl-methylxanthine) were added, ADSCs deep inside the collagen/alginate hydrogel differentiated into adipose cells gradually. More than 63% of the ADSCs differentiated into adipose cells at the end of the fourth week (Fig. 9). These data suggest that the cocktail growth factors can be delivered to the collagen/alginate loaded ADSCs through the culture medium in a controlled cascade process. This technique therefore holds the instructive significances for some other complex organ manufacturing.”

V. CONCLUSIONS

A PLGA encapsulated ADSCs/collagen/alginate 3D construct with multiple-branched channels was fabricated using a rotational combined mould system. By choosing the appropriate fabrication parameters and cell growth factors, ADSCs inside the construct maintained a high viability and differentiation rate for both endothelial and adipose cell lineages during the in vitro 4 weeks culture and engagement periods. During the earlier angiogenic growth factor engagement period ADSCs on the surface of the branched channels were much easier to differentiate into mature endothelial cells compared with those deep inside the collagen/alginate hydrogel remained their original phenotypes. During the later engagement stage, most of the ADSCs deep inside the collagen/alginate hydrogel differentiated into adipocytes. This approach might recapture the vascularization and adipogenesis processes more faithfully in a quite simple and easy manner and would be useful in complex organ, such as breast, manufacturing, drug screening and subsequent regenerative medicine.

VI. ACKNOWLEDGMENT

The Project was supported by the State Key Laboratory of Materials Processing and Die & Mould Technology, Huazhong University of Science and Technology (No. 2012-P03), the Cross-Strait Tsinghua Cooperation Basic Research (No.2012THZ02-3), the National Natural Science Foundation of China (No. 81271665 & 30970748), the National Natural



Science Foundation of China (NSFC) and Japanese Society for the Promotion of Science (JSPS) Bilateral Cooperation Program and the National High Tech 863 Grant (No. 2009AA043801).

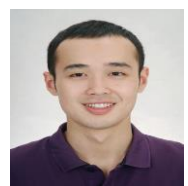
REFERENCES

- Cui T, Yan Y, Zhang R, Xu M, & Wang X. (2010). Progress in development of vascularized adipose tissues. *Journal of Mechanical Engineering*. 46:99-104.
- Wang XH. (2012). Intelligent freeform manufacturing of complex organs. *Artif Organs*. 36: 951-961.
- Wang XH, Yan YN, & Zhang RJ. (2010). Recent trends and challenges in complex organ manufacturing. *Tissue Eng Part B*.;16:189-197.
- Wang XH, Yan YN, & Zhang RJ. (2007). Rapid prototyping as a tool for manufacturing bioartificial livers. *Trends Biotechnol*. 25:505-513.
- Wang X. (2014). Spatial effects of stem cell engagement in 3D printing constructs. *J Stem Cells Res Rev & Rep*. 1; 5-9.
- Xu YF, & Wang XH. 3D biomimetic models for drug delivery and regenerative medicine. *Curr Pharm Des*, in press.
- Liu LB, Zhou XW, Xu YF, Zhang WM, Liu C-H, & Wang XH. Controlled release of growth factors for regenerative medicine. *Curr Pharm Des*, in press.
- Radisic M, Yang LM, Boublik J, Cohen RJ, Langer R, Freed LE, & Vunjak-Novakovic G. (2004). Medium perfusion enables engineering of compact and contractile cardiac tissue. *Am J Physiol Heart Circ Physiol*. 286:H507-516.
- Colton C. (1955). Implantable biohybrid artificial organs. *Cell Transplant*. 4:415-436.
- Vunjak-Novakovic G, & Scadden DT. (2011). Biomimetic platforms for human stem cell research. *Cell Stem Cell*. 8:252-261.
- Choi NW, Cabodi M, Held B, Gleghorn JP, Bonassar LJ, & Stroock AD. (2007). Microfluidic scaffolds for tissue engineering. *Nat Mater*. 6:908-915.
- Therriault D, White SR, & Lewis JA. (2003). Chaotic mixing in three-dimensional microvascular networks fabricated by direct-write assembly. *Nat Mater*. 2:265-271.
- Yeong, W-Y, Chua C-K, Leong F-F, Chandrasekaran M, & Lee M-W. (2006). Indirect fabrication of collagen scaffold based on inkjet printing technique. *Rapid Prototyping J*. 12:229-337.
- Lim D, Kamotani Y, Cho B, Mazumder J, & Takayama S. (2003). Fabrication of microfluidics mixers and artificial vasculatures using a high-brightness diode-pumped Nd:YAG laser direct write method. *Lab Chip*. 3:318-323.
- Li SJ, Xiong Z, Wang XH, Yan YN, Liu HX, & Zhang RJ. (2009). Direct fabrication of a hybrid cell/hydrogel construct via a double-nozzle assembling technology. *J Bioact Compa Polym*. 24:249-264.
- Huang YW, He K, & Wang XH. (2013). Rapid Prototyping of a hybrid hierarchical polyurethane-cell/hydrogel onstruct for regenerative medicine. *Mater Sci Eng C*. 33:3220-3229.
- Wang XH, Yan YN, & Zhang RJ. (2010). Gelatin-based hydrogels for controlled cell assembly. In: Ottenbrite RM (ed.) *Biomedical Applications of Hydrogels Handbook*. New York: Springer. 269-284.
- Wang XH, Tuomi J, Mäkitie AA, Paloheimo K-S, Partanen J, & Yliperttula M. (2013). The integrations of biomaterials and rapid prototyping techniques for intelligent manufacturing of complex organs. In: Lazinica R (ed.) *Advances in biomaterials science and applications in biomedicine*. InTech. pp437-463.
- Wang XH, & Zhang QQ. (2011). Overview on "Chinese-Finnish workshop on biomanufacturing and evaluation techniques". *Artif Organs*. 35:E191-193.
- Wang XH. (2013). Overview on biocompatibilities of implantable biomaterials. In: Lazinica R (ed.) *Advances in biomaterials science and applications in biomedicine*. InTech. 111-155.
- Risau W, Flamme I. & Vasculogenesis. (1995). *Annu Rev Cell Dev Biol*. 11:73-91.
- Stoppato M, Stevens HY, Carletti E, Migliaresi C, Motta A, & Gulberg RE. (2013). Effects of silk fibroin fiber incorporation on mechanical properties, endothelial cell colonization and vascularization of PDLLA scaffolds. *Biomaterials*. 34:4573-4581.
- Sahota PS, Burn JL, Heaton M, Freedlander E, Suvarna SK, Brown NJ, & Mac Neil S. (2003). Development of a reconstructed human skin model for angiogenesis. *Wound Repair Regen*. 11:275-284.
- Laschke MW, Strohe A, Scheuer C, Eglin D, Verrier S, Alini M, Pohlemann T, & Menger MD. (2009). *In vivo* biocompatibility and vascularization of biodegradable porous polyurethane scaffolds for tissue engineering. *Acta Biomaterialia*. 5:1991-2001.
- Kinnaird T, Stabile E, Burnett MS, Shou M, Lee CW, Barr S, Fuchs S, & Epstein SE. (2004). Local delivery of marrow-derived stromal cells augments collateral perfusion through paracrine mechanisms. *Circulation*. 109:1543-1549.
- Laschke MW, Schank TE, Scheuer C, Kleer S, Schuler S, Metzger W, Eglin D, Alini M, & Menger MD. (2013). Three-dimensional spheroids of adipose-derived mesenchymal stem cells are potent initiators of blood vessel formation in porous polyurethane scaffolds. *Acta Biomaterialia*. 9:6876-6884.
- He K, & Wang XH. (2011). Rapid prototyping of tubular polyurethane and cell/hydrogel construct. *J Bioact Compat Polym*. 26:363-374.
- Zhao XR, & Wang XH. (2013). Preparation of an adipose-derived stem cell/fibrin-poly (D, L-lactic-co-glycolic acid) construct based on a rapid prototyping technique. *J Bioact Compat Polym*. 28:191-203.
- Zhao XR, Liu LB, Wang JY, Xu YF, Zhang WM, Khang G, & Wang XH. (2014). In vitro vascularization of a combined system based on a 3D printing technique. *J Tissue Eng Regen Med*. DOI: 10.1002/term.1863.
- Bhadriraju K, & Chen CS. (2002). Engineering cellular microenvironments to improve cell-based drug testing. *DDT*. 7:612-620.
- Díaz-Prado S, Muiños-López E, Hermida-Gómez T, Fuentes-Boquete I, Esbrit P, Buján J, De Toro FJ, & Blanco FJ. (2012). Type I Collagen and heparan sulfate scaffolds support human chondrogenesis for cartilage tissue engineering. *Osteoarthritis and Cartilage*. 20:S271-272.
- Gumbiner BM. (1996). Cell adhesion: the molecular basis of tissue architecture and morphogenesis. *Cell*. 84:345-357.
- Wang XH, & Sui SC. (2011). Pulsatile culture of a poly(DL-Lactic-co-glycolic acid) sandwiched cell/hydrogel construct fabricated using a step-by-step mould/extraction methods. *Artif Organs*. 35:645-655.
- Cui TK, Yan YN, Zhang R, Liu L, Xu W, & Wang XH. (2009). Rapid prototyping a new polyurethane-collagen conduit and its Schwann cell compatibility. *J Bioact Compat Polym*. 24(S1):5-7.
- Xu W, Wang XH, Yan YN, & Zhang R. (2008). Rapid Prototyping of Polyurethane for the Creation of Vascular Systems. *J Bioact Compat Polym*. 23:103-114.
- Yan YN, Wang XH, Yin DZ, & Zhang RJ. (2007). A New Polyurethane/Heparin Vascular Graft for Small-caliber Vein Repair. *J Bioact Compat Polym*. 22:323-341.

AUTHOR PROFILE



Xiaohong Wang, Founder/Director of the Center of Organ Manufacturing, Center of Organ Manufacturing, Department of Mechanical Engineering, Tsinghua University, gotten her Ph.D. in 2001.6 in Nankai University, P. R. China, put forward a series of theories on complex organ manufacturing, awarded by the Tekes in 2011 through the Finland Distinguished Professor program (FiDiPro), published more than 40 patents, 100 articles, more than 80 of the articles are in the list of Science Citation Index (SCI). A member of the Biomanufacturing, Branch of the Mechanical Engineering Society of China, the Editorial Board of the international Journal of Bioactive and Compatible Polymers (J. Bioact. Compat. Polym., JBPCP), the World Journal of Gastrointestinal Pathophysiology (World J. Gastrointest. Pathophysiol, WJGP), the Journal of Stem Cells Research, Reviews & Reports (J. Stem Cells Res., Rev. & Rep., JSCR), a Guest Editor of the Current Pharmaceutical Design, the Current Cancer Drug Targets, the international member of the American Institute of Chemical Engineers, Biomaterials.



Jiayin Wang, gotten his B.D. in 2010 in Sichuan University, and M.E. in 2013 in Tsinghua University, P. R. China.

